INTERFACE FOCUS

rsfs.royalsocietypublishing.org

Research

Cite this article: Adamatzky A. 2018 Towards fungal computer. *Interface Focus* **8**: 20180029. http://dx.doi.org/10.1098/rsfs.2018.0029

Accepted: 4 September 2018

One contribution of 10 to a theme issue 'Computation by natural systems'.

Subject Areas:
biomathematics, biomedical engineering, computational biology

Keywords:
natural computation, fungi, unconventional computing

Author for correspondence:
Andrew Adamatzky
e-mail: andrew.adamatzky@uwe.ac.uk

THE ROYAL SOCIETY PUBLISHING

Towards fungal computer

Andrew Adamatzky

Unconventional Computing Lab, UWE, CSCT, Bristol, UK

AA, 0000-0003-1073-2662

We propose that fungi Basidiomycetes can be used as computing devices: information is represented by spikes of electrical activity, a computation is implemented in a mycelium network and an interface is realized via fruit bodies. In a series of scoping experiments, we demonstrate that electrical activity recorded on fruits might act as a reliable indicator of the fungi's response to thermal and chemical stimulation. A stimulation of a fruit is reflected in changes of electrical activity of other fruits of a cluster, i.e. there is distant information transfer between fungal fruit bodies. In an automaton model of a fungal computer, we show how to implement computation with fungi and demonstrate that a structure of logical functions computed is determined by mycelium geometry.

1. Introduction

The fungi are the largest, widely distributed and oldest group of living organisms [1]. The smallest fungi are microscopic single cells. The largest mycelium belongs to *Armillaria bulbosa*, which occupies 15 hectares and weights 10 tons [2], and the largest fruit body belongs to *Fomitiporia ellipsoidea*, which at 20 years old is 11 m long, 80 cm wide, 5 cm thick and has an estimated weight of nearly half-a-ton [3]. During the last decade, we produced nearly 40 prototypes of sensing and computing devices from the slime mould *Physarum polycephalum* [4], including the shortest path finders, computational geometry processors, hybrid electronic devices, see the compilation of the latest results in [5]. We found that the slime mould is a convenient substrate for unconventional computing; however, the geometry of the slime mould's protoplasmic networks is continuously changing, thus preventing fabrication of long-living devices, and slime mould computing devices are confined to experimental laboratory set-ups. Fungi Basidiomycetes are now taxonomically distinct from the slime mould; however, their development and behaviour are phenomenologically similar: mycelium networks are analogous to the slime mould's protoplasmic networks, and the fruit bodies are analogous to the slime mould's stalks of sporangia. Basidiomycetes are less susceptible to infections; when cultured indoors, especially commercially available species, they are larger in size and more convenient to manipulate than slime mould, and they could be easily found and experimented on outdoors. This makes the fungi an ideal object for developing future living computing devices. Advancing our recent results on electrical signalling in fungi [6], which in a way is similar to electrical signalling in plants [7], we are exploring the computing potential of fungi in the present paper. We introduce a mycelium basis of fungal computing and define an architecture of fungal computers in §2. Findings on the electrical activity of fungi [6,8,9] are augmented in §3 by demonstrations of endogenous spiking, signalling between fruit bodies and signalling by fruit bodies about the state of the growth substrate. In experiments, we use oyster mushrooms, species *pleurotus*, family Tricholomataceae, because of their wide availability and interesting properties [10–12]. We imitate electrical activity of the mycelium in a discrete model in §4. There we encode logical values into presence/absence of spikes in fruit bodies and show how logical functions can be executed. We also demonstrate that a geometrical structure of mycelium, in the model this is represented by a

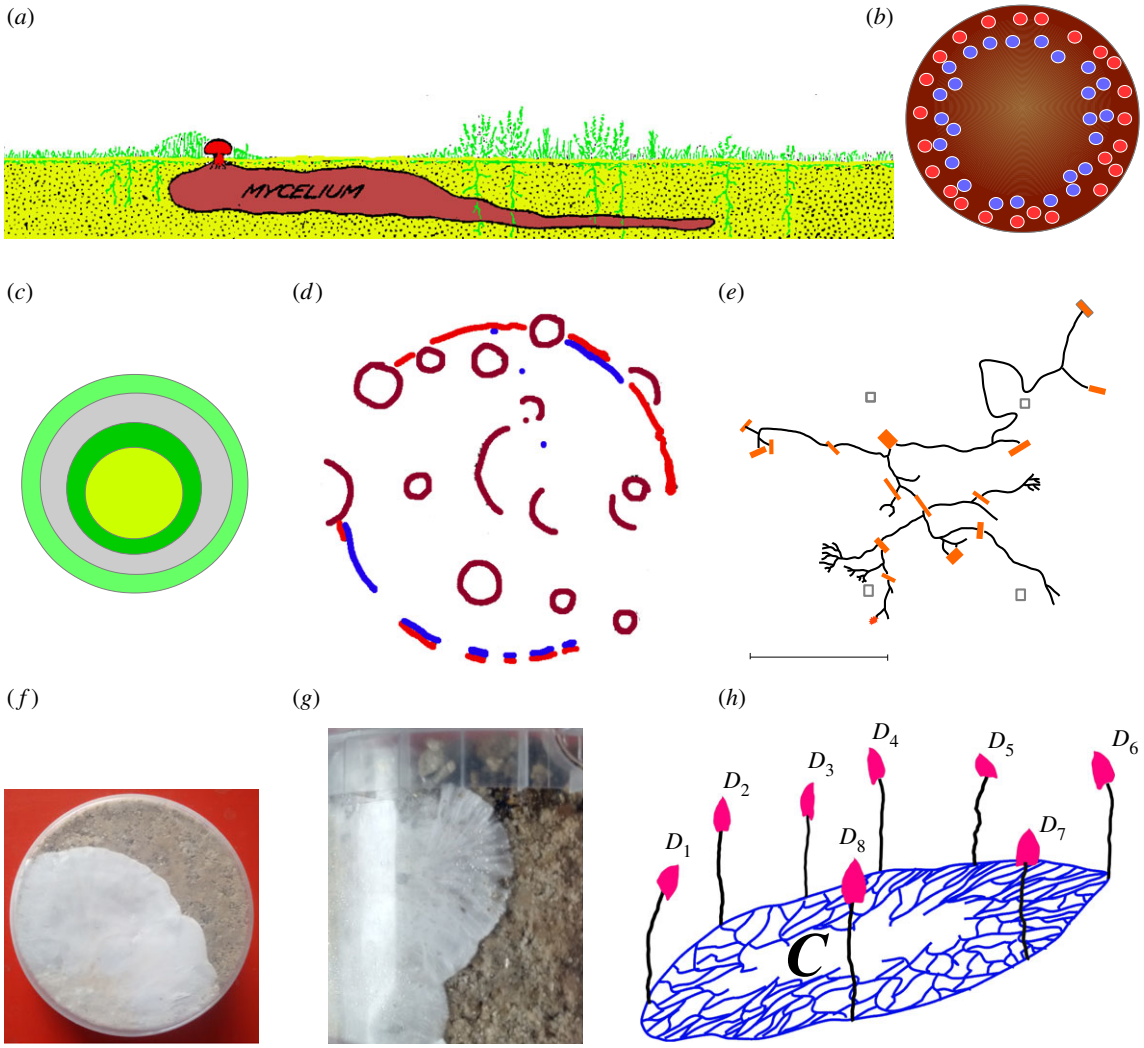

Figure 1. Development of mycelium in nutrient-rich (*a*–*d*) and nutrient-poor (*e*) substrates. (*a*) A cross-section of a fairy ring produced by *Marasmius Oreades*. Reproduced with permission from [14]. (*b*) A view from above: the mycelium is dark red, the fruits are red and the dried fruits are blue. (*c*) Vegetation profile corresponding to (*b*): outer stimulated (light green) and inner stimulated (dark green) zones of increased vegetation, dead zone (grey) of reduced vegetation and inside zone (yellow) of ambient vegetation. (*d*) Rings and fragments of rings of *Agaricus campestris* (dark red) inside 65 m ring of *Calvatia ciathyiformi* (fresh fruits are red, dry fruits are blue). Reproduced with permission from [15]. (*e*) A development pattern of a single mycelial system of *Phanerochaete velutina*. Lines are mycelial cords. Orange/grey rectangles are inoculum blocks, white rectangles decayed inoculum blocks. Scale bar, 1 m. Reproduced with permission from [16]. (*f*) Photo of mycelium propagating on a nutrient-rich cocoa substrate. (*g*) Zoomed view of the propagating front where branching is articulated. (*h*) Schematic architecture of a fungal computer. Fruit bodies D_1, D_2, . . . are I/O interface. Mycelium network ***C*** is a distributed computing device.

random planar set structure, affects families of logical circuits computed. Directions of future research on fungal computing are outlined in §5.

2. Mycelium basis of fungal computer

Mycelium propagates by a foraging front and consolidations of mycelial cords behind the front [13]. The foraging front travels outward and produces fruit bodies (figure 1*a*,*b*). The front is also manifested by rings of increased vegetation and 'exhausted' soil (figure 1*c*), see historical overviews in [14,15]. Propagation/extension of the ring is due to exhaustion of nutrients necessary for fungi growth.

A mycelial growth pattern is determined by nutritional conditions and temperature [13,17–21], as also demonstrated in computer models in [22,23]. A complexity of the mycelium network, as estimated by a fractal dimension, is determined by the nutrient availability and the pressure built up between various parts of the mycelial network [24]. In domains with high concentration of nutrients mycelia branch; in poor nutrient domains mycelia stop branching [25]. As indicated in [18] optimization of resources is evidenced by the inhibitory effect of contact with baits on the remainder of the colony margin, regression of mycelium originating from the inoculum associated with the renewed growth from the bait, and differences between growth patterns of large and small inocula/baits (figure 1*d*). Optimization of the mycelial network [20] is quite similar to that of the slime mould *P. polycephalum*, as evidenced in our previous studies, especially in terms of proximity graphs [26] and transport networks [27]. Exploration of confined spaces by hyphae has been studied in [28–32], and evidence of the efficiency of the exploration provided. All the above indicate that (i) fungal mycelium can solve the same range of computational geometry problems as the slime mould *P. polycephalum* does [5]: shortest path [33–37], Voronoi diagram [38], Delaunay triangulation, proximity graphs and spanning tree, concave hull and, possibly, convex hull, and, with some experimental efforts, the travelling salesman problem [39], and (ii) by changing environmental

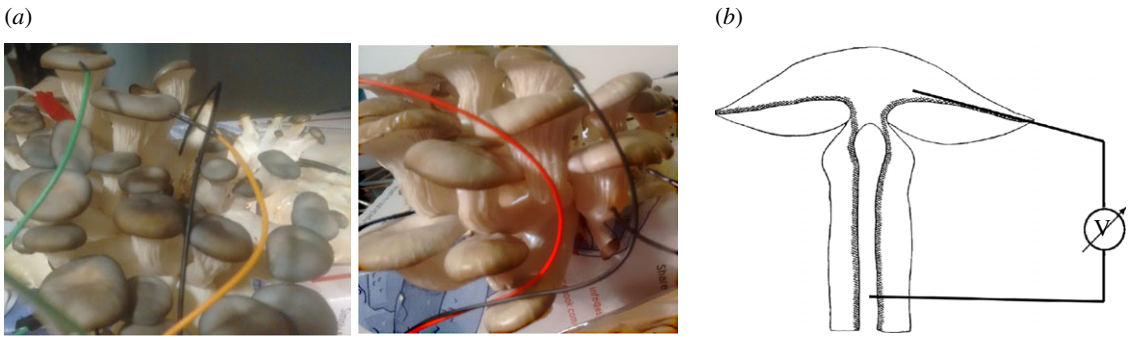

Figure 2. Experimental set-up. (*a*) Photographs of fruit bodies with electrodes inserted. (*b*) Position of electrodes in relation to a translocation zone. Drawing of fruit body is from Schütte [46]; a scheme of electrodes is ours.

conditions we can reprogram a geometry and graph-theoretical structure of the mycelium networks and then use electrical activity of fungi [6,8,9] to realize computing circuits.

A mycelium is hidden underground, therefore only configurations of fruit bodies can be seen as outputs of a geometric computation implemented by propagating mycelium. Consider the following example of interacting foraging fronts. Propagation of wavefronts of fungi at large scale was described by Shantz & Piemeisel in Yuma, Colorado, on June 1916 [15]. This is illustrated in (figure 1*d*). There are two species of fungi, *Agaricus campestris* and *Calvatia ciathyiformi*. The ring of *C. ciathyiformi* was nearly 65 m in diameter with 50 fresh fruits. There are several smaller rings of *A. campestris*: in some places, they interrupt 'wavefronts' of *C. ciathyiformi* growth. In theory, such interaction of wavefronts of different species can be used to approximate the Voronoi diagram, as has been done previously with slime mould [38,40], when planar data points are represented by locations of fungi inoculates.

Also, notice the characteristic location of dry fruits of *C. ciathyiformi* (blue in figure 1*b*,*d*); this brings in an analogy with an excitable medium: the fresh fruits are analogous to the 'excitation' wavefront and the dried fungi to 'refractory' tails of the excitation waves. Fungi rings can extend up to 200 m diameter [15]. The analogy between fungi foraging fronts and excitation wavefronts indicates that already algorithms for computing with wavefronts in excitable medium [41,42] can be realized with foraging mycelium. That said, solving geometrical problems with mycelium networks does not sound feasible, because the mycelium growth rate is very low, thus the solution of any problem could take weeks and months, if not years, for problems in which spatial representation covers hundreds of metres.

In contrast to the slow growth of mycelium, fungi exhibit an electrical response to stimulation in a matter of seconds or minutes [6,8,9]. Therefore, a computation using electrical impulses propagating in and modified by the mycelium networks seems to be promising. We propose the following architecture of a fungal computer $\mathcal{A}$ (figure 1*h*): a mycelium $\mathbf{C}$ is a processor, or rather a network of processors, and fruit bodies $D_1, D_2, \ldots$ comprise I/O interface of the fungal computer. The information is represented by spikes of electrical potential. Thus, a state of D_i^t at a time step t could be either binary, depending on whether a spike is present or absent at time t, or multiple valued, depending on a number of spikes in a train, duration of spikes and their amplitudes. Any fruit body can be considered as input and output and the fungal computer $\mathcal{A}$: $\mathbf{D}^{t+w} = \mathcal{F}(\mathbf{D})$, where w is a positive integer. Details on how exactly $\mathcal{A}$ could compute will be analysed in §4; first let us consider, §3, a few examples from laboratory experiments on endogenous spiking, response of fungi to stimulation and evidence of communication between fruit bodies.

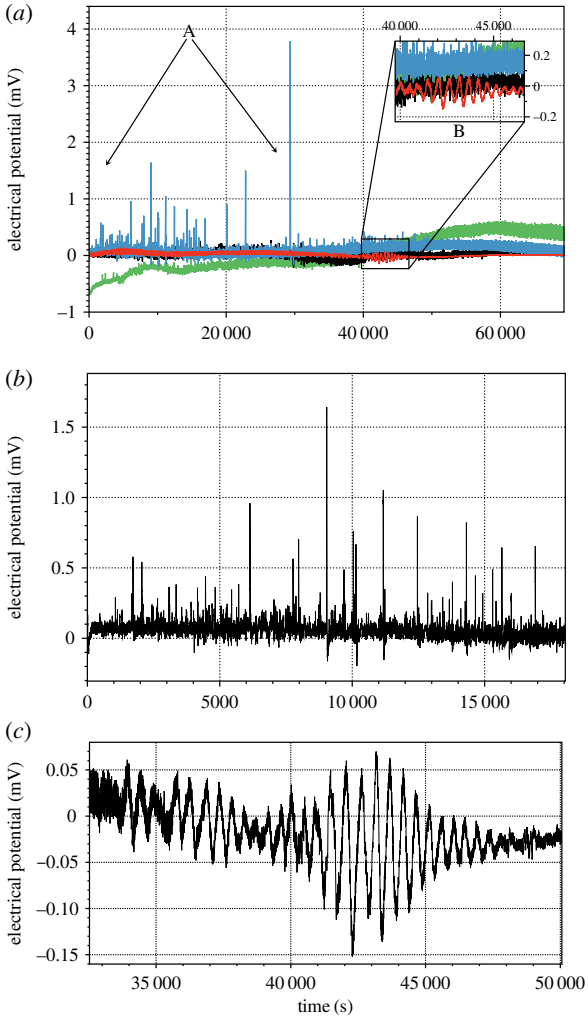

Figure 3. Co-existence of various types of electrical activity in fruit bodies of the same cluster. (*a*) Electrical potential recorded for over 16 h on four fruits. (*b*) Zoomed in area marked 'A' in (*a*). Large amplitude spikes. (*c*) Zoomed in area marked 'B' in (*a*). Two wave-packets.

3. Electrical activity of fungi

3.1. Experimental procedure

We used commercial mushroom growing kits[1] of pearl oyster mushrooms *P. ostreatus*. In the experiments reported seven

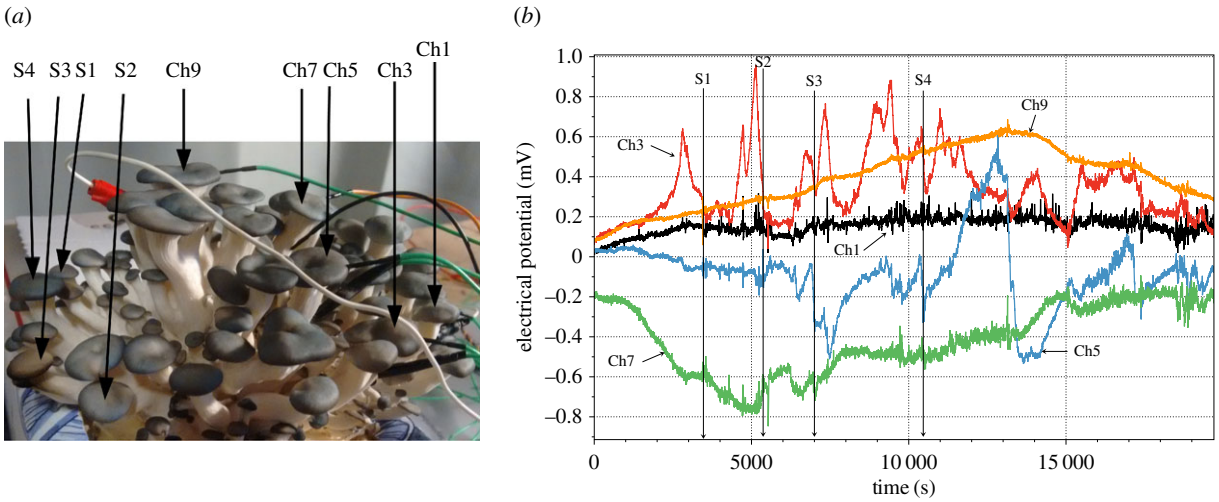

Figure 4. Stimulation of fruits. (*a*) Set-up of recording, sites of stimulation and location of electrode pairs corresponding to channels Ch1–Ch9. (*b*) Electrical potential recording on five mushrooms. Channel Ch1 is shown by black, Ch3 red, Ch5 blue, Ch7 green and Ch9 orange. The following stimuli have been applied to fruiting bodies. (S1) 3450 s: start open flame stimulation for 20 s. (S2) 5310 s: start open flame stimulation for 60 s. (S3) 7000 s: ethanol drop is placed on a cap of the fruit. (S4) 10440 s: 15 mg of table salt is placed on a cap of one of fruiting bodies.

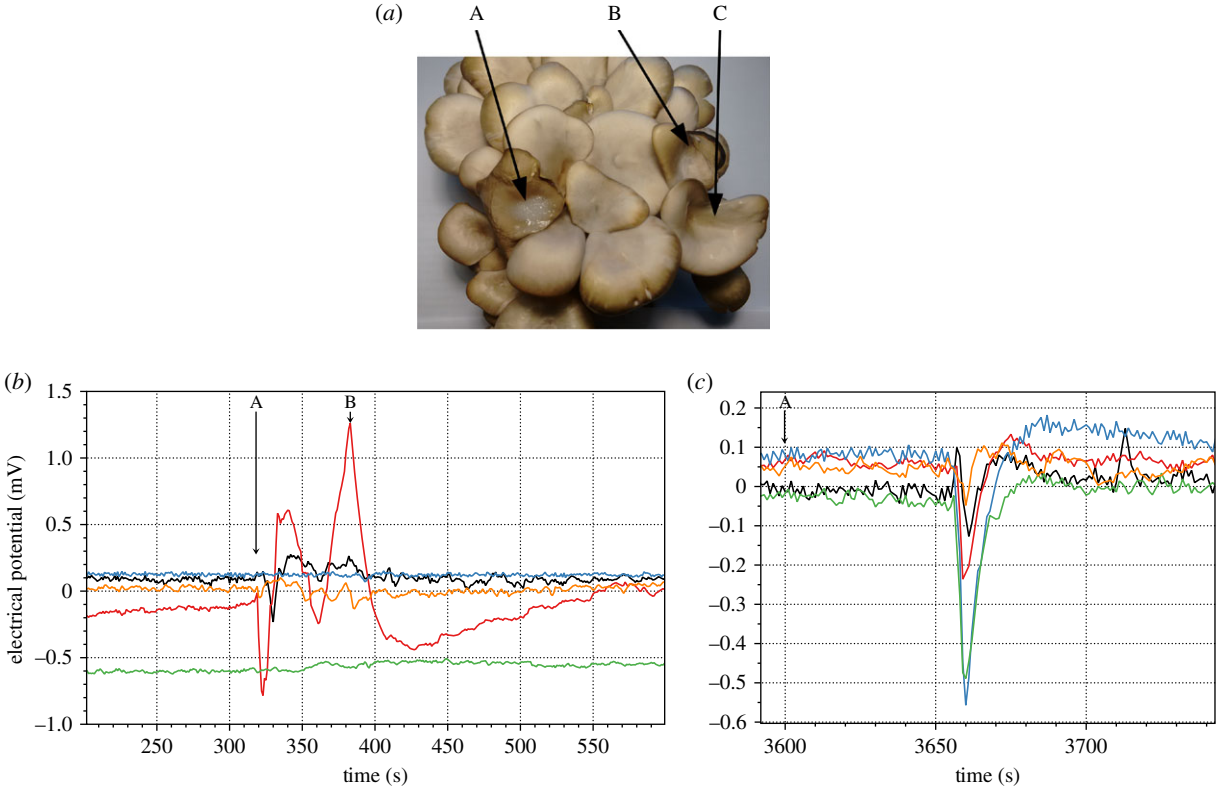

Figure 5. Response of fruits to stimulation of neighbouring fruits. (*a*) Photo of the fruit cluster taken *after* experiments were completed. The stimulated fruits are indicated by arrows: 20 mg of salt (A), open flame of a butane lighter, temperature 600–800°C for 60 s (B), 20 mg sugar (C). (*b*) Electrical potential of five non-stimulated fruits during stimulation of a fruit from their cluster with an open flame: start of the thermal stimulation is shown by arrow 'A', end of the stimulation by arrow 'B'. (*c*) Electrical potential of five fruits recorded during stimulation of a fruit from their cluster with salt, moment when salt was placed on a cap is shown by arrow labelled 'A'.

growing kits were used. For each kit, we recorded electrical activity of the first flush of fruiting bodies only because the first flush usually provides the maximum yield of fruiting bodies [43] and the growing mycelium in the substrate was less affected by products of fungi metabolism [44,45]. Each substrate's bag was 22 cm × 10 cm × 10 cm, 800–900 g in weight. The bag was cross-sliced 10 cm vertical and 8 cm horizontal and placed in a cardboard box with 8 cm × 10 cm opening. Experiments were conducted at room temperature in constant (24 h) ambient lighting of 10 lux. Electrical potential of fruit bodies was recorded from the second to third day of their emergence. Resistance between cap and stalk of a fruit body was 1.5 MΩ on average between any two heads in the cluster 2 MΩ (measured by Fluke 8846 A). We recorded the electrical potential difference between cap and stalk of the fruit body. We used sub-dermal needle electrodes with twisted cable.[2] A recording electrode was inserted into the stalk and a reference electrode in the translocation zone; figure 2*b* shows

the cross-section of a fruit body showing the translocation zone, drawing by Schütte [46], of the cap; the distance between electrodes was 3–5 cm. In each cluster, we recorded four to six fruit bodies simultaneously (figure 2*a*) for 2–3 days. Electrical activity of fruit bodies was recorded with an ADC-24 High-Resolution Data Logger.[3] The data logger employs differential inputs, galvanic isolation and software-selectable sample rates—these contribute to a superior noise-free resolution; its 24-bit A/D converter maintains a gain error of 0.1%. Its input impedance is 2 MΩ for differential inputs, and offset error is 36 µV in ±1250 mV range use. We recorded the electrical activity one sample per second; during the recording the logger made as many measurements as possible (typically up 600) per second then saved the average value.

3.2. Endogenous spiking

As we previously discussed in [6] fruits show a rich family of endogenous, i.e. not caused by purposeful stimulation during experiments, spiking behaviour. Spiking patterns of several types have been observed during simultaneous recording from the different fruits of the same cluster. Recordings of four fruit bodies during nearly 20 h are shown in figure 3. Most pronounced patterns are the trains of large amplitude spikes (figure 3*b*) and the wave-packets (figure 3*c*).

Large amplitude spikes (figure 3*b*) have average amplitude 0.77 mV, s.d. 0.29. The spikes are usually observed in pairs. Average distance between spikes in a pair is 238 s, s.d. 81 s. Time interval between the two largest, over 0.8 mV, spikes varies from 20 to 48 min. Two wave-packets are shown in figure 3*c*. The first wave-packet, roughly 91 min long, consists of 10 spikes. Their amplitude varies from 0.05 mV at the beginning to 0.1 mV at the eclipse. The shortest spike is 362 s duration; the longest, in the middle of the waveform, is 705 s. The second most pronounced wave-packet consists of 19 spikes and lasts for 163 min. Amplitudes of the spikes vary from 0.05 mV at the beginning of the wave-packet to 0.2 mV in the middle. The shortest spike is 457 s long, and the longest spike is 609 s long. Average spike duration is 516 s ($\sigma = 56$); average amplitude is 0.12 mV ($\sigma = 0.06$).

3.3. Signalling between fruits

To check if fruits in a cluster would respond to stimulation of their neighbours, we conducted the experiments illustrated in figure 4. Note, fruits which electrical potential recorded were not stimulated (figure 4*a*). Recording on one of the fruiting bodies (Ch3) shows periodic oscillations: average amplitude 0.47 mV ($\sigma = 0.19$), average duration of a spike is 1669 s (s.d. 570) and average period 1819 s (s.d. 847) (figure 4*b*). Other recorded fruiting bodies also show substantial yet non-periodic changes in the electrical potential with amplitudes up to 1 mV. A thermal stimulation, S1 and S2, in figure 4*b*, leads to a temporal disruption of oscillation of the fruit Ch3, and low-amplitude short-period spikes in other recorded fruits Ch1, Ch2, Ch4–Ch9. The response of an intact fruit to stimulation of another fruit with an open flame consists of a depolarization approximately 0.02 mV amplitude, approximately 6 s duration, followed by a repolarization approximately 0.2 mV amplitude, approximately 9 s duration. The depolarization starts approximately 3 s after start of stimulation. This might indicate that it is caused by action potential-like fast dynamical changes. High-amplitude repolarization takes place at approximately 13 s after start of stimulation, when a substantial loci of a fruit

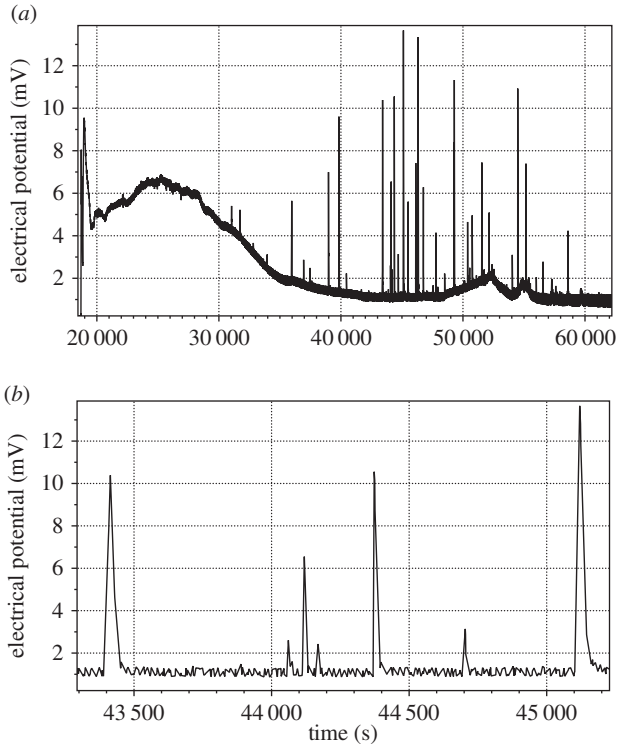

Figure 6. Electrical response of a fruit body to the injection of saline solution in the substrate.

cap becomes thermally damaged. Application of ethanol (S3, figure 4) and salt (S4, figure 4) leads to a 0.15–0.45 mV drop in electrical potential; recovery occurs in approximately 1200 s.

In the experiment illustrated in figure 5, we stimulated fruits with an open flame, salt and sugar, and recorded electrical responses from non-stimulated neighbours. Application of sugar did not cause any response, and thus can be seen as a control experiment on mechanical stimulation. No responses to a short-term (approx. 1–2 s) mechanical stimulation were recorded. Fruits respond to thermal stimulation of a member of their cluster by a couple of action-potential like impulses (figure 5*b*). The amplitude of the response differs from fruit to fruit, and more likely depends not only on the distance between the recorded fruit and the stimulated fruit but also on the position of electrodes. The fruits respond to saline stimulation of their neighbour in a more uniform manner (figure 5*c*). In 12–15 s after the application of salt, the electrical potential of the recorded fungi drops by approximately 0.2,−0.8 mV. The potential recovers in approximately 30 s.

3.4. Signalling about state of growth substrate

To test the response of fruits to environmental changes in the growth substrate, we injected 150 ml of sodium chloride (6 mg ml^{-1}) in the substrate and recorded the electrical potential of a fruit. The moment of injection is reflected in the spike of electrical potential with amplitude 9 mV. This spike might be caused by mechanical stimulation of mycelium (figure 6). Four hours after injection, the recorded fruit exhibited trains of spiking activity. Amplitude of spikes vary from 0.29 to 12.3 mV, average 4.1 mV ($\sigma = 3.5$ mV). Duration of a spike varies from 33 s to 151 s, average 71 s ($\sigma = 32$ s). Periods vary from 450 s to 2870 s, average duration 953 s ($\sigma = 559$). The spikes might be caused by an osmotic function of mycelium due to intake of saline solution and transported into the caps of fruits [47] (cited by Gallé *et al*. [7]).

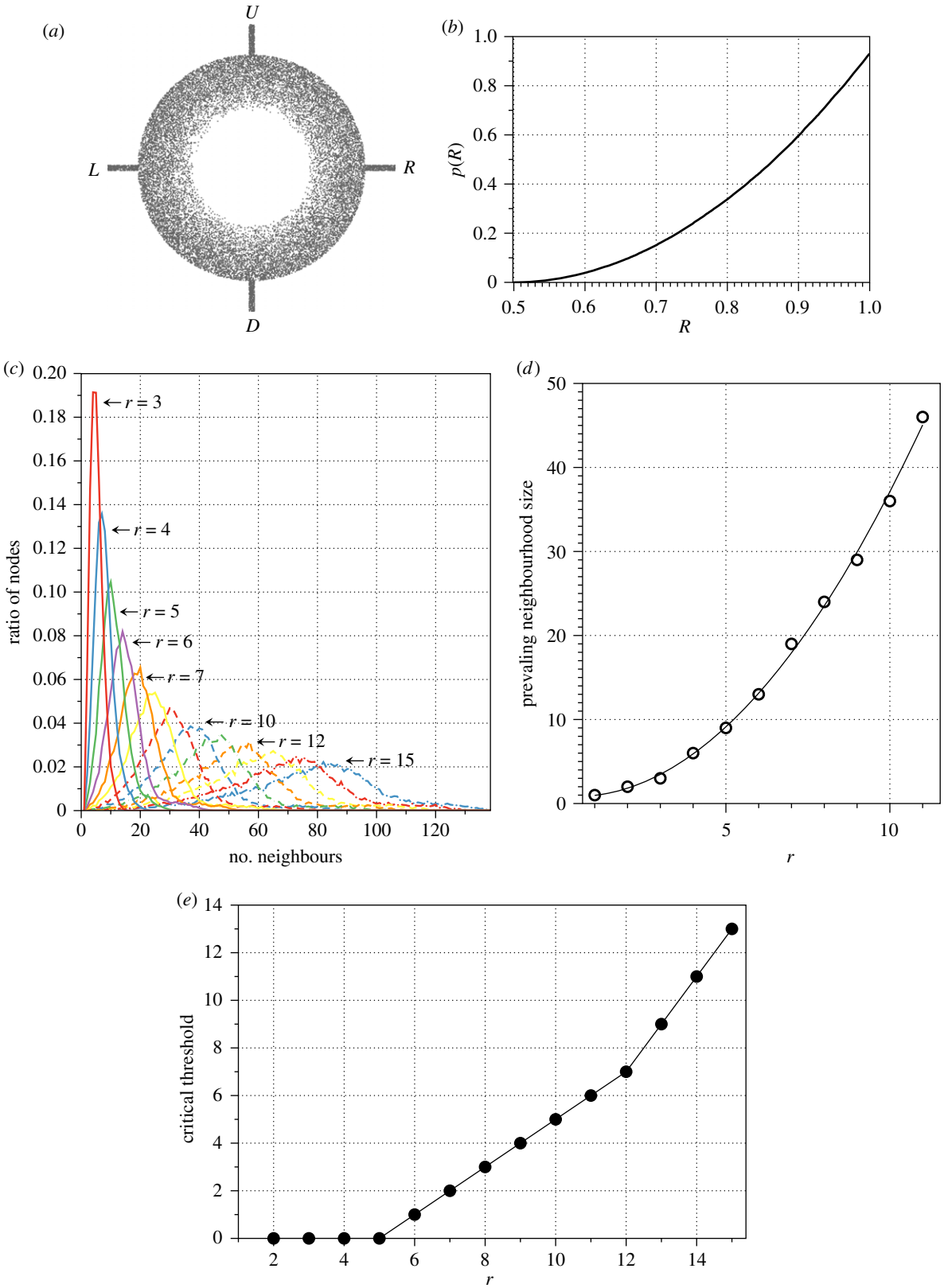

Figure 7. Fungal computer architecture. (*a*) Visualization of **C**. (*b*) Probability of point in **C** as a function of distance from *R*. (*c*) Distribution of a number of neighbours for $r = 3 \ldots 15$. A number of neighbours depending on a neighbourhood radius *r*. (*d*) Prevailing number of neighbours for $r = 3 \ldots 15$. (*e*) Critical values of excitation threshold θ for $r = 1, \ldots, 15$.

4. Automaton model of a fungal computer

To imitate propagation of depolarization waves in the mycelium network, we adopt an automaton model. The automaton models are proved to be appropriate discrete models for spatially extended excitable media [48–50] and verified in models of calcium wave propagation [51], propagation of electrical pulses in the heart [52–54] and simulation of action potential [55,56]. We represent a fungal computer by an automaton $\mathcal{A} = \langle \mathbf{C}, \mathbf{Q}, r, h, \theta, \delta \rangle$, where $\mathbf{C} \subset \mathbf{R}$ is a planar set, each point $p \in \mathbf{C}$ takes states from the set $\mathbf{Q} = \{\bigstar, \bullet, \circ\}$, excited ($\bigstar$), refractory ($\bullet$), resting ($\circ$), and updates its state in a discrete time depending on its current state and state of its neighbourhood $u(p) = \{q \in \mathbf{C} : d(p, q) \leq r\}$; r is a neighbourhood radius, θ is an excitation threshold and δ is refractory

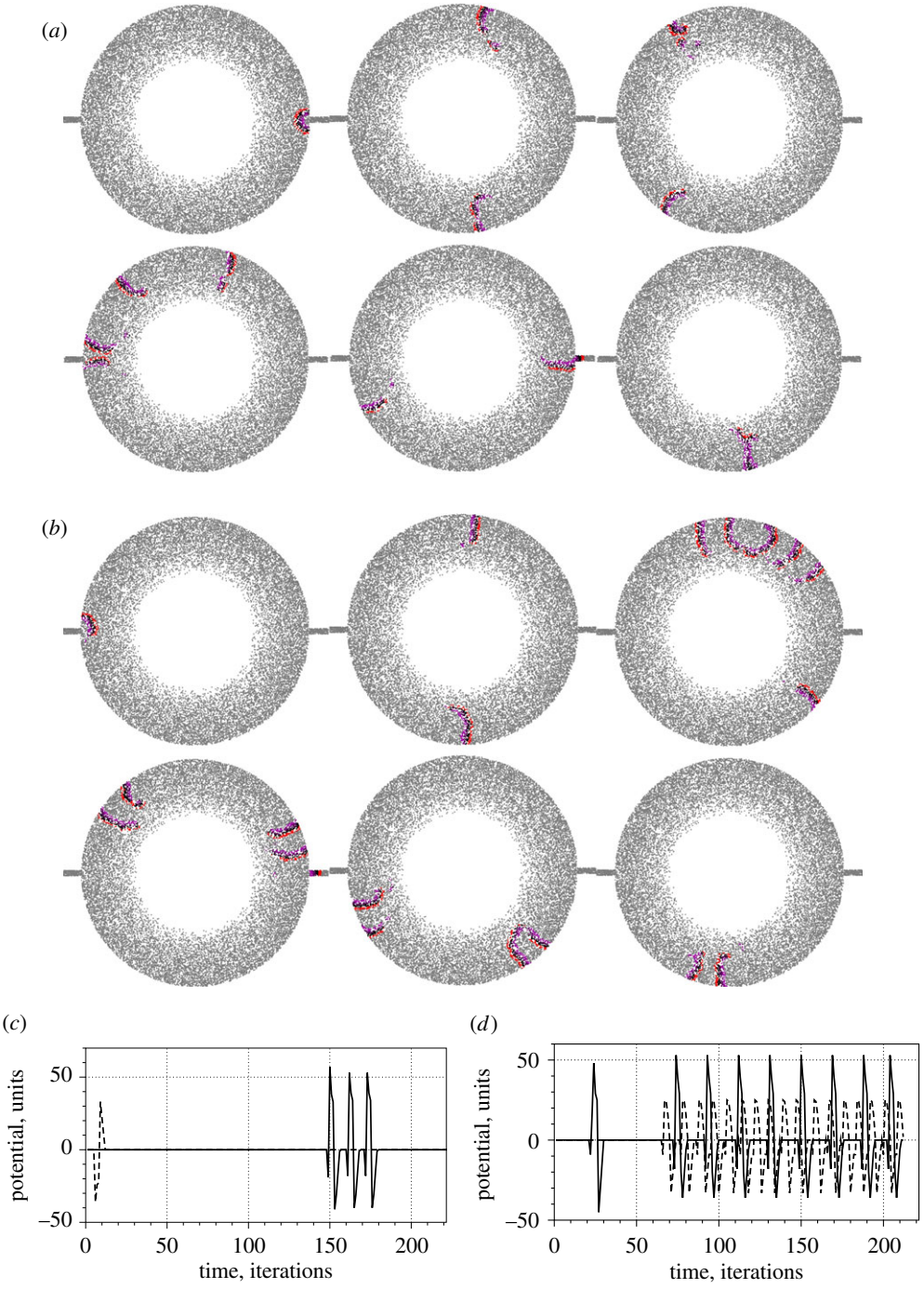

Figure 8. Dynamics of the excitation of two fruit automaton $\mathcal{A}$: in scenarios of right R (*a*,*c*) and left L (*b*,*d*) fruits excited. (*a*,*b*) Exemplar snapshots of the dynamics. (*c*,*d*) Electrical potential measured. Dashed line is a potential measured on R and solid line is a potential measured on L.

delay. All points update their states in parallel and by the same rule:

$$p^{t+1}\begin{cases}\bigstar, & \text{if } (p^t=\circ) \text{ and } \sigma(p)^t>\theta\\ \bullet, & \text{if } (p^t=\circ) \text{ or } ((p^t=\bullet) \text{ and } (h_p^t>0))\\ \circ, & \text{otherwise}\end{cases}$$

$$h_p^{t+1}=\begin{cases}\delta, & \text{if } (p^{t+1}=\bullet) \text{ and } (p^t=\bigstar)\\ h_p^t-1, & \text{if } (p^{t+1}=\bullet) \text{ and } h_p^t>0\\ 0, & \text{otherwise.}\end{cases}$$

Every resting ($\circ$) point of **C** excites ($\bigstar$) at the moment $t+1$ if a number of its excited neighbours at the moment t—$\sigma(p)^t=|\{q\in u(p): q^t=\bigstar\}|$—exceeds a threshold θ. Excited point $p^t=\bigstar$ takes refractory state $\bullet$ at the next time step $t+1$, at the same moment a counter of refractory state h_p is set to the refractory delay δ. The counter is decremented, $h_p^{t+1}=h_p^t-1$ at each iteration until it becomes 0. When the counter h_p becomes zero the point p returns to the resting state $\circ$.

Architecture of **C** was chosen as follows. We randomly distributed 2×10^4 points in a ring with small radius $R=0.5$ and large radius 1 (figure 7*a*). To reflect the higher density of mycelium near the propagation front and decay of mycelium inside the propagating disc we distributed points with a probability described by a quadratic function $p(R)=3.7\cdot R^2-3.6\cdot R+0.9$, where $R\in[0.5,1]$ (figure 7*b*); the function reflects biomass distribution in a cross-section of a fairy ring [57,58]. To imitate fruit bodies, we distributed points in horizontal (L and R) and vertical (U and D) domains with size 0.27 by 0.023 (figure 7*a*); each domain contains 370 points distributed randomly. Distributions of a point's number of neighbours for neighbourhood radius $r=3,\ldots,15$ are shown

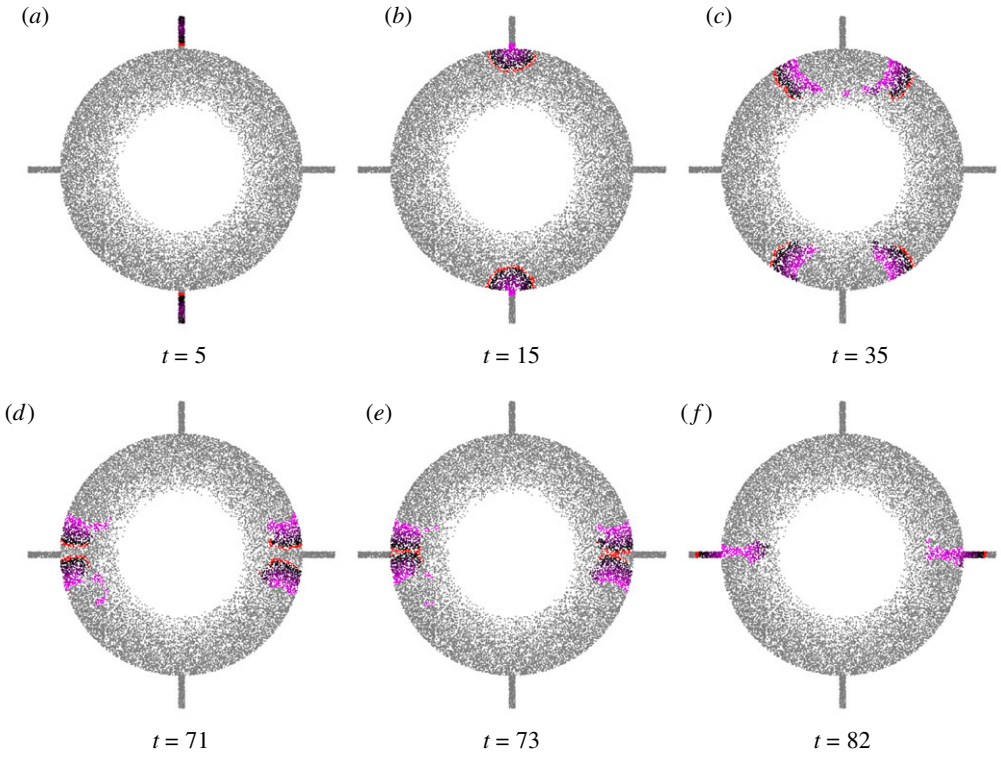

Figure 9. (*a–f*) Snapshots of excitation dynamics in a four-fruit fungal automaton for inputs $R = 0$, $U = 1$, $D = 0$, $L = 1$.

in figure 7*c*. We have chosen $\theta = 4$ (§4.2.1), $\theta = 5$ (§4.2.2), $r = 10$, $\delta = 5$ in the reported experiments for the following reasons. A median radius $r = 10$ neighbourhood size is approximately 600 times less than a number of points in **C** (figure 7*d*); thus a locality of the automaton state updates is assured. Excitation threshold $\theta = 4$ is critical for $\mathcal{A}$ with $r = 10$ (figure 7*e*), i.e. it assures that excitation wavefronts propagate for at least half of the perimeter of the ring (figure 7*a*).

4.1. Automaton action potential

The automaton $\mathcal{A}$ supports propagation of excitation waves, fronts of which are represented by points in the state ★ and tails by points in state •. We assume a point in the state ★ has higher electrical potential than a point in the state •. To imitate a voltage difference between electrodes inserted in fruit bodies we select two domains, D_1 and D_2, in each of four fruit bodies and calculate a voltage difference V between domains as follows: $V = \sum_{q \in D_1} \chi(q^t) - \sum_{q \in D_2} \chi(q^t)$, where $\chi(\circ) = 0$, $\chi(\bigstar) = 1$, and $\chi(\bullet) = h_q^t$. This imitates an electrical potential difference between electrodes inserted in the cap and the step of a fruit, as illustrated in figure 2.

We excite the fungal automaton $\mathcal{A}$ by assigning points of a selected fruit body states ★. This is equivalent to thermal or mechanical stimulation of fruits in our laboratory experiments. We record voltage on fruit bodies at every iteration of the automation evolution. Two examples are shown in figure 8. For simplicity, we consider $\mathcal{A}$ with only two fruit bodies: L and R. When right fruit R is stimulated (see first spike in figure 8*c*) an excitation wave propagates into the mycelium ring **C** and splits into two waves (figure 8*a*). Excitation waves enter fruit bodies when they reach them, which is reflected in spikes of the calculated potential. If the medium was regular (as e.g. a lattice) the excitation wavefronts would annihilate each other when colliding. However, the disorganized structure of the conductive medium leads to formation of the new excitation waves (see train of three spikes in figure 8*c*). New waves travel along the ring but eventually die out. Excitation of the left fruit L (figure 8*b*) generate two waves propagating along the ring. However, in this case, due to irregularity of the excitable medium a temporary wave generator is born in the upper part of the ring (2nd snapshot in figure 8*b*). The generator produces pairs of waves (3rd snapshots in figure 8*b*). The transition from sparse spiking to wave-packets is similar to experimental results shown in figure 3. In this example, we witness that fungal responses to stimulation of the left and the right fruits are different. This can be employed in designs of computing schemes with fungal automata, as outlined in the next section.

4.2. Logical functions computed by $\mathcal{A}$

Dynamics of excitation wave propagation and interaction in **C** is determined by exact configuration of the planar set. The configurations are generated at random; therefore we expect fungal automaton to implement different functions for each, or nearly, configuration. This is illustrated by the two following examples. Here we use four fruit bodies acting as both inputs and outputs. A logical input TRUE, or '1', is represented by excitation of a chosen fruit body. A logical output TRUE, or '1', is recognized as one or more impulses recorded at the fruit body some time interval after stimulation: we started recording 40 iterations (the parameter w introduced in §2) of automaton evolution, after stimulation and stopped recording 130 iterations. Let us consider two examples. The sets **C** are generated randomly, therefore the dynamics of excitation is expected to be different in these examples.

4.2.1. First example

In the first example, we consider the configuration **C** shown in figure 9*a*. Excitation dynamics for inputs $R = 0$, $U = 1$, $D = 0$, $L = 1$ is shown in figure 9 and for inputs $R = 1$, $U = 0$, $D = 1$, $L = 0$ in figure 10. When fruits U and D are stimulated

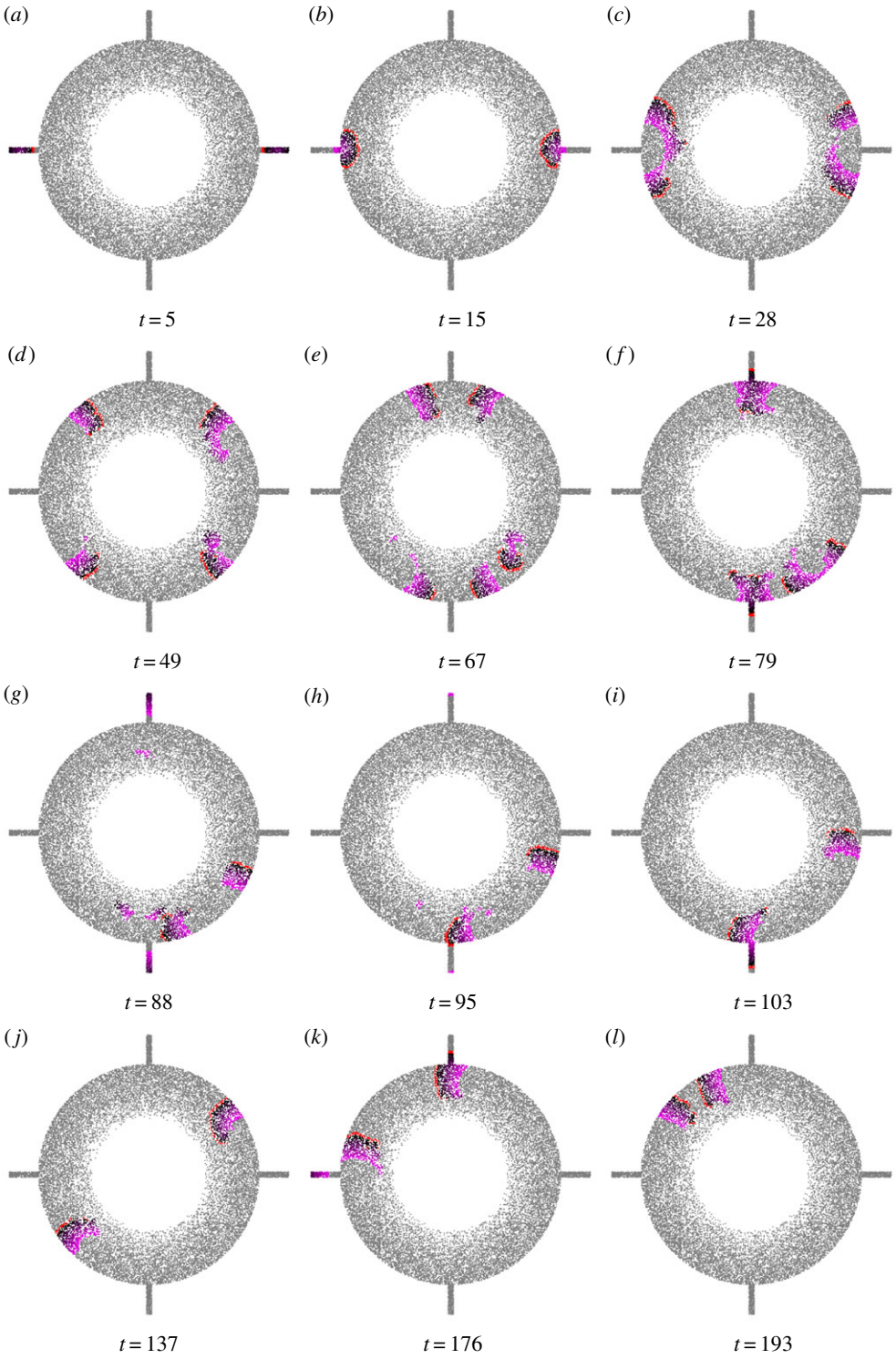

Figure 10. (*a–l*) Snapshots of excitation dynamics in a four-fruit fungal automaton for inputs $R = 1$, $U = 0$, $D = 0$, $L = 1$.

(figure 9) the fungal automaton $\mathcal{A}$ responds with spikes on fruits L and R (figure 11*a*). Excitation dynamics is less trivial when fruits L and R are stimulated (figure 10): automaton $\mathcal{A}$ responds with two voltage spikes at fruit D, and a single spike at fruits U and R (figure 11*b*). When only fruit R is stimulated the automaton $\mathcal{A}$ responds with pairs of spikes on all fruits but L (figure 12*b*). The automaton $\mathcal{A}$ responds with a spike on fruit L just before cut-off time 150. After the 150th iteration, two centres of spiral waves are formed and thus the fungal automaton exhibits regular trains of spikes on all fruit bodies (figure 12*a*), similar to the dynamics of excitation shown in figure 4*b*.

We stimulated the fungal automaton with 16 combinations of input variables and constructed a tabular representation of a function realized by the automaton (table 1), where R, U, L, D are values of input variables, and $R^\star$, $U^\star$, $L^\star$, $D^\star$ are values of output variables. Assuming one or two impulses on the fruits represent TRUE we have the following functions implemented by the fungal automaton:

$$\left.\begin{aligned} R^\star &= \bar{R}(U + L + D) + R\bar{D}, \\ U^\star &= \bar{U}(L + U + R), \\ L^\star &= \bar{L}(D + U + R) \\ \text{and} \qquad D^\star &= \bar{D}(L + U + R), \end{aligned}\right\} \tag{4.1}$$

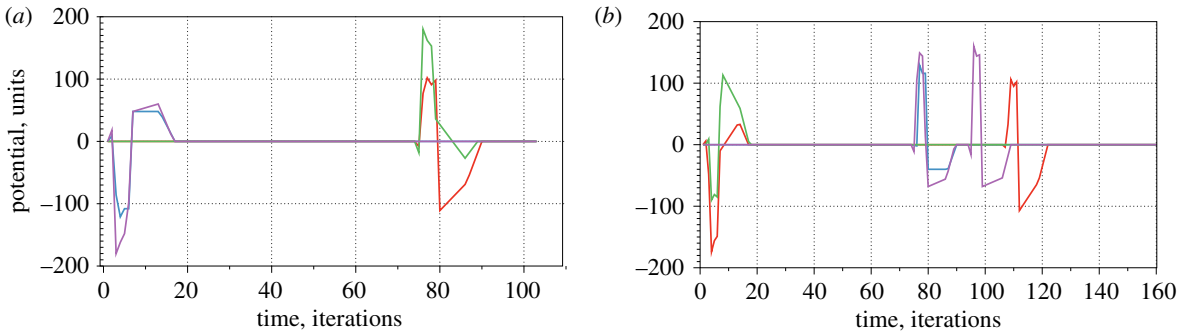

Figure 11. Voltage measured on four fruits for inputs (*a*) $R = 0$, $U = 1$, $D = 0$, $L = 1$, see dynamics in figure 9, and (*b*) $R = 1$, $U = 0$, $D = 1$, $L = 0$, see dynamics in figure 10. Voltage recorded on fruit R is plotted with red colour, U blue, L green and D magenta.

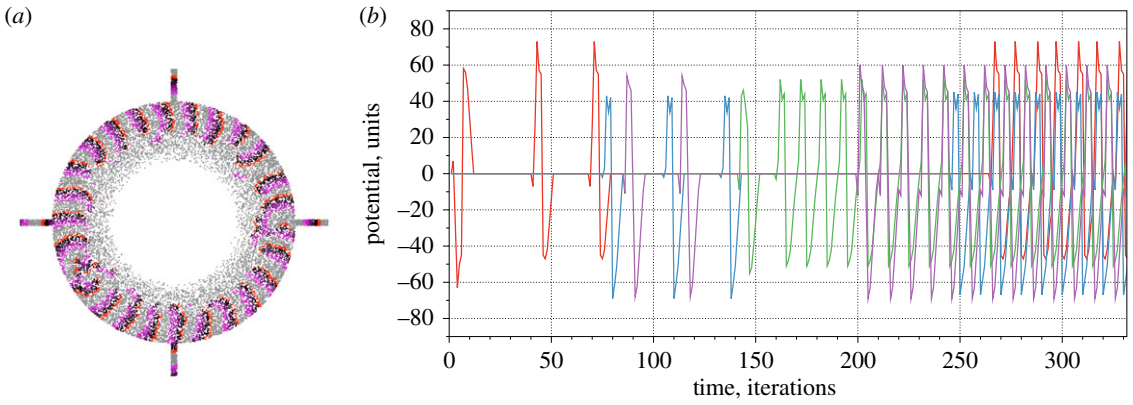

Figure 12. Response of the fungal automaton for input values $R = 1$, $U = 0$, $D = 0$, $L = 0$. (*a*) A snapshot of the automaton taken at 350th step of evolution. (*b*) Voltage recorded on the fruit R is plotted with red colour, U blue, L green and D magenta.

Table 1. Table of a function realized by four-fruit automaton $\mathcal{A}$ (figure 9*a*). One impulse on a fruit is shown by '1', two impulses by '2' and no impulses by '0'.

R	U	L	D	$R^\star$	$U^\star$	$L^\star$	$D^\star$
0	0	0	0	0	0	0	0
0	0	0	1	1	1	1	0
0	0	1	0	1	1	0	1
0	0	1	1	1	1	0	0
0	1	0	0	1	0	1	1
0	1	0	1	1	0	1	0
0	1	1	0	1	0	0	1
0	1	1	1	1	0	0	0
1	0	0	0	1	1	1	2
1	0	0	1	0	1	1	0
1	0	1	0	1	1	0	2
1	0	1	1	0	1	0	0
1	1	0	0	1	0	1	2
1	1	0	1	0	0	1	0
1	1	1	0	1	0	0	2
1	1	1	1	0	0	0	0

with the equivalent circuit for fruit D shown in figure 13. If we assume that only two impulses represent TRUE we have $R^\star = U^\star = L^\star = 0$ and $D^\star = R\bar{D}$.

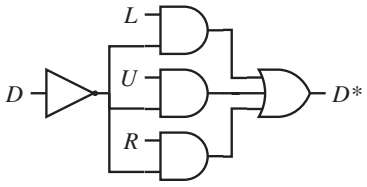

Figure 13. Equivalent logical circuit for fruit D implemented by the fungal automaton $\mathcal{A}$, with configuration of **C** shown in figure 9*a*.

4.2.2. Second example

In the second example, discussed below, we used a random configuration of points $\mathbf{C}^4$ and the automaton $\mathcal{A}$ with $\delta = 5$, $r = 10$ and $\theta = 5$. Frames and videos of the experiments are available at https://drive.google.com/open?id=1XSTQt7lD2KGUHCuJchJ–ah6CO-XUSap. Dynamics of electrical potential for 15 combinations of input values is shown in figure 14. The response of the automaton is illustrated in table 2. Assuming one impulse or two impulses on the fruits symbolize '1', we have the following functions realized on each of the fruit bodies:

$$\left.\begin{aligned} R^\star &= 0, \\ U^\star &= L + D, \\ L^\star &= \bar{L}D(R + U) + R\bar{U}L\bar{D} \\ \text{and} \qquad D^\star &= L(\bar{R} + D + U). \end{aligned}\right\} \tag{4.2}$$

Assuming only two impulses on the fruits symbolize '1', we have the following functions recorded on each of the

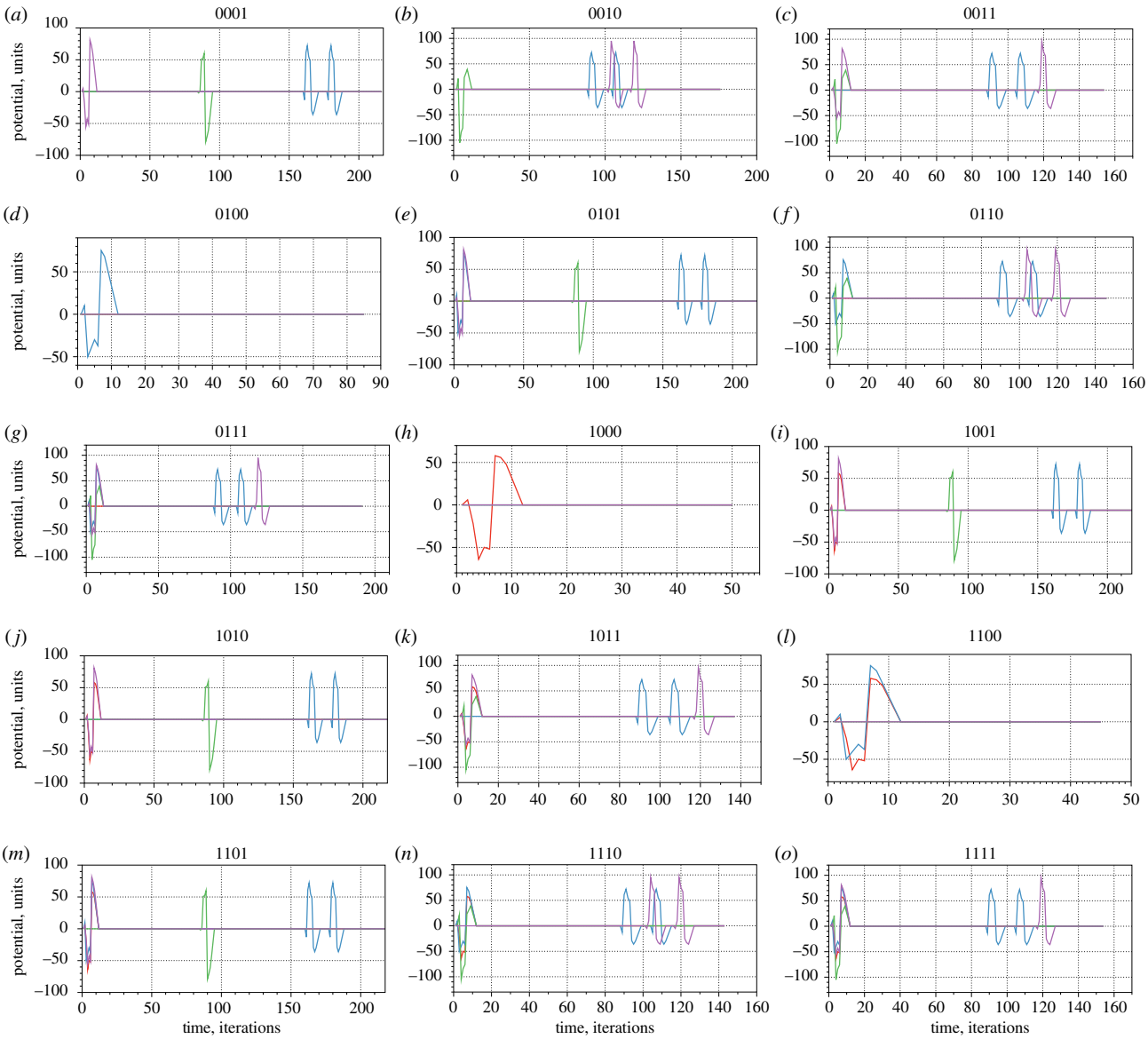

Figure 14. (*a*–*o*) Dynamics of electrical potential on fruits, in experiment with random seed 357556317, in response to stimulation of inputs. The inputs are shown in the captions in the format (*RULD*). Spikes appearing during first 10–15 iterations are input spikes. All other spikes are outputs. Voltage recorded on fruit *R* is plotted with red colour, *U* blue, *L* green and *D* magenta.

fruit bodies:

$$\left.\begin{aligned} R^\star &= 0,\\ U^\star &= L + D(R + U),\\ L^\star &= R\bar{U}\,\bar{L}D\\ \text{and}\qquad D^\star &= L\bar{D}(\bar{R} + U). \end{aligned}\right\} \tag{4.3}$$

5. Discussion

We proposed that fungi can be used as computing devices: information is represented by spikes of electrical activity, a computation is implemented in a mycelium network and an interface is realized via fruit bodies. In laboratory experiments, we demonstrated that fungi respond with spikes of electrical potential to stimulation of their fruit bodies. Thus, we can input data into a fungal computer via mechanical, chemical and electrical stimulation of the fruit bodies. Electrical signalling in fungi, previously evidenced during intracellular recording of electrical potential [8,9], is similar to the signalling in plants [7,59]. The experimental results provided in the paper are of illustrative nature with focus on architectures of potential computing devices; a statistical analysis of spontaneous spiking behaviour of the fungi can be found in [6]. Further extensive studies will be necessary to obtain statistical results on fungal response to a stimulation, particularly on the response's dependence on a strength of stimuli and inter-species differences in their responses.

Voltage spikes travelling along mycelium networks might be seen as analogous, but of different physical and chemical nature, to oxidation wavefronts in a thin-layer Belousov–Zhabotinsky (BZ) medium [60,61]. Thus, in future, we could draw some useful designs of fungal computers based on an established set of experimental laboratory prototypes of BZ computing devices. The prototypes produced are image processes and memory devices [62–64], logical gates implemented in geometrically constrained BZ medium [65,66], approximation of shortest path by excitation waves [67–69], memory in BZ microemulsion [64], information coding with frequency of oscillations [70], on-board controllers for robots [71–73], chemical diodes [74,75], neuromorphic architectures [42,76–80] and associative

Table 2. Table of a logical function realized by four-fruit automaton $\mathcal{A}$. One impulse on a fruit is shown by '1', two impulses by '2' and no impulses by '0'.

R	*U*	*L*	*D*	$R^\star$	$U^\star$	$L^\star$	$D^\star$
0	0	0	0	0	0	0	0
0	0	0	1	0	2	1	0
0	0	1	0	0	2	0	2
0	0	1	1	0	2	0	1
0	1	0	0	0	0	0	0
0	1	0	1	0	2	1	0
0	1	1	0	0	2	0	2
0	1	1	1	0	2	0	1
1	0	0	0	0	0	0	0
1	0	0	1	0	2	2	0
1	0	1	0	0	2	1	0
1	0	1	1	0	2	0	1
1	1	0	0	0	0	0	0
1	1	0	1	0	2	1	0
1	1	1	0	0	2	0	2
1	1	1	1	0	2	0	1

memory [81,82], wave-based counters [83] and other information processors [84–87]. First steps have been already made towards prototyping arithmetical circuits with BZ: simulation and experimental laboratory realization of gates [41,65,66,88–90], clocks [91] and evolving logical gates [92]. A one-bit half-adder, based on a ballistic interaction of growing patterns [93], was implemented in a geometrically constrained light-sensitive BZ medium [94]. Models of multi-bit binary adder, decoder and comparator in BZ are proposed in [95–98]. These architectures employ crossover structures as T-shaped coincidence detectors [99] and chemical diodes [75] that heavily rely on heterogeneity of geometrically constrained space. By controlling excitability [100] in different loci of the medium, we can achieve impressive results, as it is demonstrated in works related to analogues of dendritic trees [79], polymorphic logical gates [101], and experimental laboratory prototype of four-bit input, two-bit output integer square root circuits based on alternating 'conductivity' of junctions between channels [102].

Spikes of electrical potential are not the only means of implementing information processing in fungal computers. Microfluidics could be an additional computational resource. Eukaryotic cells, including slime moulds and fungi, exhibit cytoplasmic streaming [103,104]. In experiments with the slime mould *P. polycephalum*, we found that when a fragment of protoplasmic tube is mechanically stimulated, cytoplasmic streaming in this fragment halts and the fragment's resistance substantially increases. Using this phenomenon, we designed a range of logical circuits and memory devices [105]. These designs can be adopted in prototypes of fungal computers; however, more experiments would be necessary to establish optimal ways of mechanical addressing of strands of mycelium.

5.1. Programmability

To program fungal computers, we must control the geometry of the mycelium network. The geometry of the mycelium network can be modified by varying nutritional conditions and temperature [13,21–23], especially the degree of branching is proportional to the concentration of nutrients [25], and a wide range of chemical and physical stimuli [106]. Also, we can geometrically constrain it [28–32]. The feasibility of shaping similar networks has been demonstrated in [107]: high-amplitude, high-frequency voltage applied between two electrodes in a network of protoplasmic tubes of *P. polycephalum* leads to abandonment of the stimulated protoplasmic without affecting the non-stimulated tubes and low-amplitude, low-frequency voltage applied between two electrodes in the network enhances the stimulated tube and encourages abandonment of other tubes [107].

5.2. Parameters of fungal computers

Interaction of voltage spikes, travelling along mycelium strands, at the junctions between strands is a key mechanism of fungal computation. We can see each junction as an elementary processor of a distributed multi-processor computing network. We assume the number of junctions is proportional to the number of hyphal tips. There are estimated to be 10–20 tips per 1.5–3 mm [108] of a substrate. Without knowing the depth of the mycelial network, we go for the safest lower margin of two-dimensional estimation: 50 tips mm^{-2}. Considering that the largest known fungi, *Armillaria bulbosa*, populates over 15 hectares [2], we could assume that there could be 75×10^{11} branching points, that is nearly a trillion of elementary processing units. With regards to a speed of computation by fungal computers, Olsson & Hansson [9] estimated that electrical activity in fungi could be used for communication with message propagation speed 0.5 mm s^{-1} (this is several orders slower than the speed of a typical action potential in plants: from 0.005 mm s^{-1} to 0.2 mm s^{-1} [109]). Thus, it would take about half an hour for a signal in the fungal computer to propagate 1 m. The low speed of signal propagation is not a critical disadvantage of potential fungal computers, because they never meant to compete with conventional silicon devices.

5.3. Application domains

Likely application domains of fungal devices could be large-scale networks of mycelium which collect and analyse information about environment of soil and, possibly, air and execute some decision-making procedures. Fungi 'possess almost all the senses used by humans' [106]. Fungi sense light, chemicals, gases, gravity and electric fields. Fungi show a pronounced response to changes in a substrate pH [110], demonstrate mechanosensing [111]; they sense toxic metals [112], CO_2 [113] and direction of fluid flow [114]. Fungi exhibit thigmotactic and thigmomorphogenetic responses, which might be reflected in dynamic patterns of their electrical activity [115]. Fungi are also capable of sensing chemical cues, especially stress hormones, from other species [116], thus they might be used as reporters of health and well-being of other inhabitants of the forest. Thus, fungal computers can be made an essential part of distributed large-scale environmental sensor networks in ecological research to assess not just soil quality but the overall health of the ecosystems [117–119].

5.4. Further studies

In automaton models of a fungal computer, we have shown that a structure with Boolean functions realized depends on

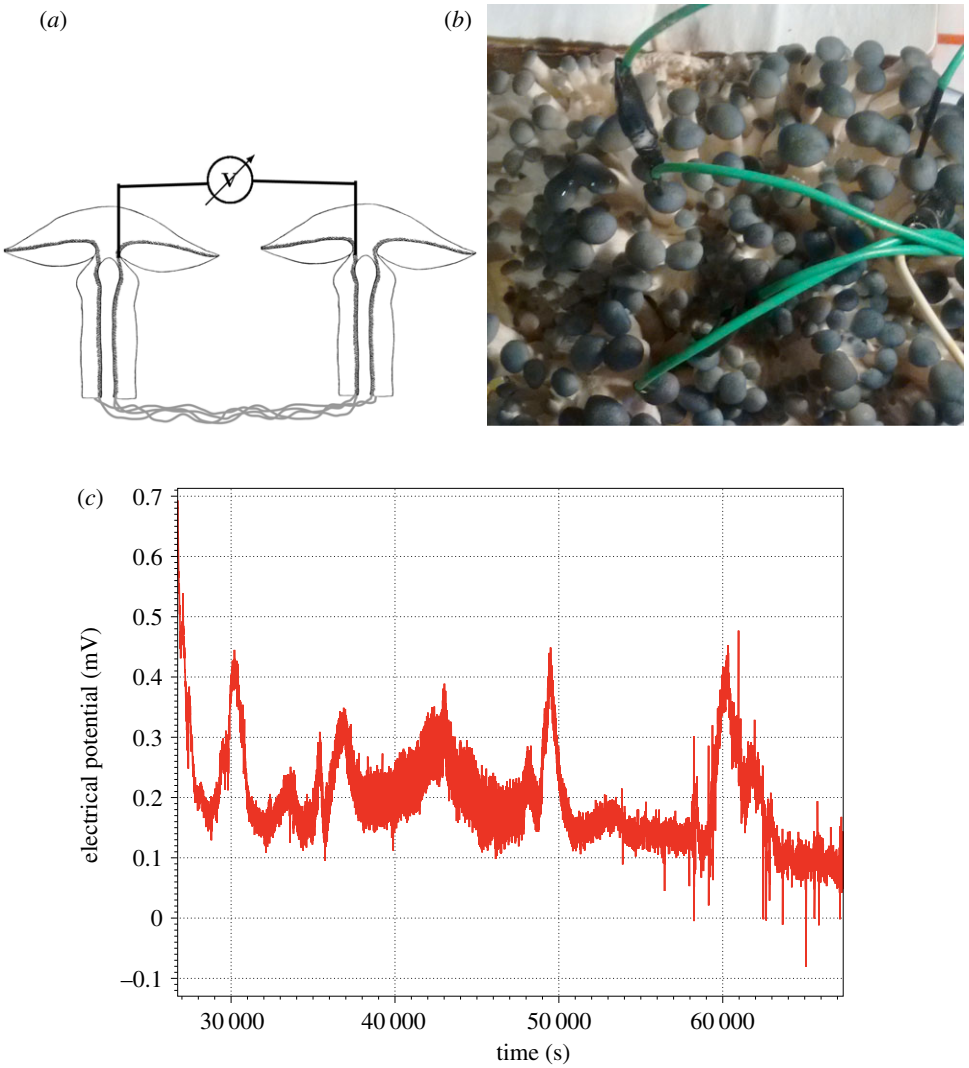

Figure 15. Electrical potential difference between two neighbouring fruits. (*a*) Position of electrodes when measuring potential different between fungal bodies. (*b*) Part of experimental set-up. (*c*) Exemplar plot of electrical potential.

the geometry of a mycelial network. In further studies, we will tackle four aspects of fungal computing as follows.

First, ideas developed in the automaton model of a fungal computer should be verified in laboratory experiments with fungi. In the automaton model developed, we did not take into account a full range of parameters recorded during experimental laboratory studies: origination and propagating of impulses have been imitated in the dynamics of the final state machines. To keep the same physical nature of inputs and outputs, we will consider stimulating fruit bodies with alternating electrical current. To cascade logical circuits implemented in clusters of fruit bodies, we might need to include amplifiers in the hybrid fungi-based electrical circuits.

Second, in experiments we evidenced electrical responses of fruits to thermal and chemical stimulation; in some cases, we observed trains of spikes. This means we could, in principle, apply experimental findings of Physarum oscillatory logic [120], where logical values are represented by different types of stimuli, apply threshold operations to frequencies of the electrical potential oscillations, and attempt to implement logical gates. Another option would be to adopt ideas of oscillatory threshold logic reported in [121]; however, this might require unrealistically precise control of the geometry of mycelial networks.

Third, we might consider measuring electrical potential between fungal bodies. In the set-up shown in figure 15*a*,*b*,

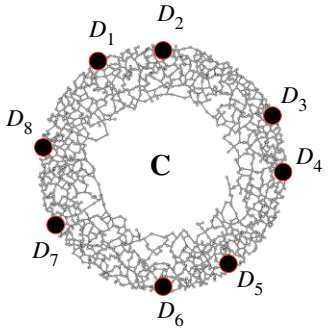

Figure 16. Representation of a mycelium by relative neighbourhood graph with 2000 nodes. Black discs are fruit bodies.

we recorded the electrical potential difference between neighbouring fruits. An example of the recorded activity is shown in figure 15*b*. Average distance between spikes is 4111 s ($\sigma = 2140$). Average duration of a spike is 287 s ($\sigma = 1515$). Average amplitude is 0.25 mV ($\sigma = 0.06$). There is a possibility that patterns of oscillation will be affected by stimulation of other fruit bodies in the cluster. This might lead to a complementary method of computing with fungi.

Fourth, we must learn how to programme the geometry of mycelial networks to be able to execute not arbitrary, as demonstrated in the automaton model, but predetermined

logical circuits. The computer modelling approach may be based on formal representation of mycelial networks as a proximity graph, e.g. relative neighbourhood graph [122] (figure 16), and then dynamically updating the graph structure till a desired logical circuit is implemented on the graph. Connection rules in proximity graphs are fixed, therefore the graph structure can be updated only by adding or removing nodes. A new set of nodes can be added to a living mycelial network by placing sources of nutrients. However, due to the very slow growth rate of mycelium, this could be unfeasible. Thus, the best way would be to focus only on removing parts of the mycelial network. When parts of a network are removed the network will re-route locally, and the set of logical functions implemented by the network will change.

Data accessibility. Videos of computer experiments are accessible at https://doi.org/10.5281/zenodo.1451496.

Competing interests. I declare I have no competing interests.

Funding. I received no funding for this study.

Acknowledgements. I acknowledges pearl oyster mushrooms *P. ostreatus* for their cooperation in the studies.

Endnotes

[1]Copyright © Espresso Mushroom Company, Brighton, UK.
[2]Copyright © SPES MEDICA SRL Via Buccari 21 16153 Genova, Italy.
[3]Pico Technology, St Neots, Cambridgeshire, UK.
[4]File with coordinates is available here https://drive.google.com/open?id=1wcmo8DkcKN49rDSRFGm9hnIjJj5LTbDL.

Reference

1. Carlile MJ, Watkinson SC, Gooday GW. 2001 *The fungi*. Utrecht, The Netherlands: Gulf Professional Publishing.
2. Smith ML, Bruhn JN, Anderson JB. 1992 The fungus *Armillaria bulbosa* is among the largest and oldest living organisms. *Nature* **356**, 428. (431doi:10.1038/356428a0)
3. Dai Y-C, Cui B-K. 2011 *Fomitiporia ellipsoidea* has the largest fruiting body among the fungi. *Fungal Biol.* **115**, 813–814. (doi:10.1016/j.funbio.2011.06.008)
4. Adamatzky A. 2010 *Physarum machines: computers from slime mould*, vol. 74. Singapore: World Scientific.
5. Adamatzky A. 2016 *Advances in Physarum machines: sensing and computing with slime mould*. Berlin, Germany: Springer.
6. Adamatzky A. 2018 On spiking behaviour of oyster fungi *Pleurotus djamor*. *Sci. Rep.* **7873**, 7873. (doi:10.1038/s41598-018-26007-1)
7. Gallé A, Lautner S, Flexas J, Fromm J. 2015 Environmental stimuli and physiological responses: the current view on electrical signalling. *Environ. Exp. Bot.* **114**, 15–21. (doi:10.1016/j.envexpbot.2014.06.013)
8. Slayman CL, Scott Long W, Gradmann D. 1976 'Action potentials' in Neurospora crassa, a mycelial fungus. *Biochim. Biophys. Acta* **426**, 732–744. (doi:10.1016/0005-2736(76)90138-3)
9. Olsson S, Hansson BS. 1995 Action potential-like activity found in fungal mycelia is sensitive to stimulation. *Naturwissenschaften* **82**, 30–31. (doi:10.1007/BF01167867)
10. Royse DJ. 1997 Speciality mushrooms and their cultivation. *Hortic. Rev.* (*Am. Soc. Hortic. Sci*) **19**, 59–97. (doi:10.1002/9780470650622.ch2)
11. Khan MA, Tania M. 2012 Nutritional and medicinal importance of Pleurotus mushrooms: an overview. *Food Rev. Int.* **28**, 313–329. (doi:10.1080/87559129.2011.637267)
12. Thorn RG, Barron G.L. 1984 Carnivorous mushrooms. *Science* **224**, 76–78. (doi:10.1126/science.224.4644.76)
13. Boddy L, Wells JM, Culshaw C, Donnelly DP. 1999 Fractal analysis in studies of mycelium in soil. *Geoderma* **88**, 301–328. (doi:10.1016/S0016-7061(98)00111-6)
14. Marin Molliard M. 1910 De l'action du Marasmius oreades fr. sur la végétation. *Bulletin De La Societe Botanique De France* **57**, 62–69. (doi:10.1080/00378941.1910.10832167)
15. Shantz HL, Piemeisel RL. 1917 Fungus fairy rings in eastern Colorado and their effects on vegetation. *J. Agric. Res.* **XI**, 191–245.
16. Dowson CG, Rayner ADM, Boddy L. 1988 Inoculation of mycelial cord-forming basidiomycetes into woodland soil and litter II. Resource capture and persistence. *New Phytologist* **109**, 343–349. (doi:10.1111/j.1469-8137.1988.tb04204.x)
17. Watkinson SC. 1975 The relation between nitrogen nutrition and formation of mycelial strands in *Serpula lacrimans*. *Trans. Br. Mycol. Soc.* **64**, 195–200. (doi:10.1016/S0007-1536(75)80102-1)
18. Dowson CG, Rayner ADM, Boddy L. 1986 Outgrowth patterns of mycelial cord-forming basidiomycetes from and between woody resource units in soil. *Microbiology* **132**, 203–211. (doi:10.1099/00221287-132-1-203)
19. Jennings DH. 1995 *The physiology of fungal nutrition*. Cambridge, UK: Cambridge University Press.
20. Boddy L, Hynes J, Bebber DP, Fricker MD. 2009 Saprotrophic cord systems: dispersal mechanisms in space and time. *Mycoscience* **50**, 9–19. (doi:10.1007/S10267-008-0450-4)
21. Thi Hoa H, Wang C-L. 2015 The effects of temperature and nutritional conditions on mycelium growth of two oyster mushrooms (*Pleurotus ostreatus* and *Pleurotus cystidiosus*). *Mycobiology* **43**, 14–23. (doi:10.5941/MYCO.2015.43.1.14)
22. Rayner ADM. 1991 The challenge of the individualistic mycelium. *Mycologia* **83**, 48–71. (doi:10.1080/00275514.1991.12025978)
23. Regalado CM, Crawford JW, Ritz K, Sleeman BD. 1996 The origins of spatial heterogeneity in vegetative mycelia: a reaction-diffusion model. *Mycol. Res.* **100**, 1473–1480. (doi:10.1016/S0953-7562(96)80080-3)
24. Bolton RG, Boddy L. 1993 Characterization of the spatial aspects of foraging mycelial cord systems using fractal geometry. *Mycol. Res.* **97**, 762–768. (doi:10.1016/S0953-7562(09)80158-5)
25. Ritz K. 1995 Growth responses of some soil fungi to spatially heterogeneous nutrients. *FEMS Microbiol. Ecol.* **16**, 269–279. (doi:10.1111/j.1574-6941.1995.tb00291.x)
26. Adamatzky A. 2009 Developing proximity graphs by *Physarum polycephalum*: does the plasmodium follow the toussaint hierarchy? *Parallel. Process. Lett.* **19**, 105–127. (doi:10.1142/s0129626409000109)
27. Adamatzky A (ed.). 2012 *Bioevaluation of world transport networks*. Singapore: World Scientific.
28. Hanson KL, Nicolau Jr L, Filipponi DV, Wang L, Lee AP, Nicolau DV. 2006 Fungi use efficient algorithms for the exploration of microfluidic networks. *Small* **2**, 1212–1220. (doi:10.1002/smll.200600105)
29. Held M, Edwards C, Nicolau DV. 2008 Examining the behaviour of fungal cells in microconfined mazelike structures. In *Imaging, manipulation, and analysis of biomolecules, cells, and tissues VI* (eds DL Farkas, DV Nicolau, RC Leif), vol. 6859, p. 68590U. Bellingham, WA: International Society for Optics and Photonics.
30. Held M, Edwards C, Nicolau DV. 2009 Fungal intelligence; or on the behaviour of microorganisms in confined micro-environments. *J. Phys. Conf. Ser.*, **178**, 012005. (doi:10.1088/1742-6596/178/1/012005)
31. Held M, Lee AP, Edwards C, Nicolau DV. 2010 Microfluidics structures for probing the dynamic behaviour of filamentous fungi. *Microelectron. Eng.* **87**, 786–789. (doi:10.1016/j.mee.2009.11.096)
32. Held M, Edwards C, Nicolau DV. 2011 Probing the growth dynamics of neurospora crassa with microfluidic structures. *Fungal. Biol.* **115**, 493–505. (doi:10.1016/j.funbio.2011.02.003)
33. Nakagaki T, Yamada H, Tóth Á. 2000 Intelligence: maze-solving by an amoeboid organism. *Nature* **407**, 470. (doi:10.1038/35035159)
34. Nakagaki T. 2001 Smart behavior of true slime mold in a labyrinth. *Res. Microbiol.* **152**, 767–770. (doi:10.1016/s0923-2508(01)01259-1)
35. Nakagaki T, Yamada H, Toth A. 2001 Path finding by tube morphogenesis in an amoeboid organism. *Biophys. Chem.* **92**, 47–52. (doi:10.1016/s0301-4622(01)00179-x)

36. Nakagaki T, Iima M, Ueda T, Nishiura Y, Saigusa T, Tero A, Kobayashi R, Showalter K. 2007 Minimum-risk path finding by an adaptive amoebal network. *Phys. Rev. Lett.* **99**, 068104. (doi:10.1103/PhysRevLett.99.068104)
37. Tero A, Takagi S, Saigusa T, Ito K, Bebber DP, Fricker MD, Yumiki K, Kobayashi R, Nakagaki T. 2010 Rules for biologically inspired adaptive network design. *Science* **327**, 439–442. (doi:10.1126/science.1177894)
38. Shirakawa T, Adamatzky A, Gunji Y-P, Miyake Y. 2009 On simultaneous construction of voronoi diagram and delaunay triangulation by physarum polycephalum. *Int. J. Bifurcation Chaos* **19**, 3109–3117. (doi:10.1142/S0218127409024682)
39. Jones J, Adamatzky A. 2014 Computation of the travelling salesman problem by a shrinking blob. *Nat. Comput.* **13**, 1–16. (doi:10.1007/s11047-013-9401-x)
40. Jones J, Adamatzky A. 2015 Slime mould inspired generalised Voronoi diagrams with repulsive fields. (http://arxiv.org/abs/1503.06973)
41. Adamatzky A. 2004 Collision-based computing in Belousov–Zhabotinsky medium. *Chaos Solitons Fractals* **21**, 1259–1264. (doi:10.1016/j.chaos.2003.12.068)
42. Gorecki J, Natalia Gorecka J, Igarashi Y. 2009 Information processing with structured excitable medium. *Nat. Comput.* **8**, 473–492. (doi:10.1007/s11047-009-9119-y)
43. Shah ZA, Ashraf M, Ishtiaq M. 2004 Comparative study on cultivation and yield performance of oyster mushroom (pleurotus ostreatus) on different substrates (wheat straw, leaves, saw dust). *Pakistan J. Nutr.* **3**, 158–160. (doi:10.3923/pjn.2004.158.160)
44. Sánchez C. 2010 Cultivation of *pleurotus ostreatus* and other edible mushrooms. *Appl. Microbiol. Biotechnol.* **85**, 1321–1337. (doi:10.1007/s00253-009-2343-7)
45. Oei P. 2003 *Mushroom cultivation: appropriate technology for mushroom growers*, 3rd edn. Backhuys Publishers.
46. Schütte KH. 1956 Translocation in the fungi. *New Phytologist* **55**, 164–182. (doi:10.1111/j.1469-8137.1956.tb05278.x)
47. Mummert H, Gradmann D. 1976 Voltage dependent potassium fluxes and the significance of action potentials in *Acetabularia*. *Biochim. Biophys. Acta* **443**, 443–450. (doi:10.1016/0005-2736(76)90464-8)
48. Markus M, Hess B. 1990 Isotropic cellular automaton for modelling excitable media. *Nature* **347**, 56–58. (doi:10.1038/347056a0)
49. Gerhardt M, Schuster H, Tyson JJ. 1990 A cellular automation model of excitable media including curvature and dispersion. *Science* **247**, 1563–1566. (doi:10.1126/science.2321017)
50. Weimar JR, Tyson JJ, Watson LT. 1992 Diffusion and wave propagation in cellular automaton models of excitable media. *Physica D: Nonlinear Phenomena* **55**, 309–327. (doi:10.1016/0167-2789(92)90062-R)
51. Lechleiter J, Girard S, Peralta E, Clapham D. 1991 Spiral calcium wave propagation and annihilation in xenopus laevis oocytes. *Science* **252**, 123–126. (doi:10.1126/science.2011747)
52. Saxberg BEH, Cohen RJ. 1991 Cellular automata models of cardiac conduction. In *Theory of heart* (eds L Glass, P Hunter, A McCulloch), pp. 437–476. Berlin Germany: Springer.
53. Dowle M, Mantel RM, Barkley D. 1997 Fast simulations of waves in three-dimensional excitable media. *Int. J. Bifurcation Chaos* **7**, 2529–2545. (doi:10.1142/S0218127497001692)
54. Siregar P, Sinteff JP, Julen N, Le Beux P. 1998 An interactive 3D anisotropic cellular automata model of the heart. *Comput. Biomed. Res.* **31**, 323–347. (doi:10.1006/cbmr.1998.1485)
55. Ye P, Entcheva E, Grosu R, Smolka SA. 2005 Efficient modeling of excitable cells using hybrid automata. In *Proc. of CMSB*, vol. 5, pp. 216–227. Berlin, Germany: Springer.
56. Alonso Atienza F, Requena Carrión J, García Alberola A, Rojo Álvarez JL, Sánchez Muñoz JJ, Martínez Sánchez J, Valdés Chávarri M. 2005 A probabilistic model of cardiac electrical activity based on a cellular automata system. *Revista Española de Cardiología* (*English Edition*) **58**, 41–47. (doi:10.1016/S1885-5857(06)60233-8)
57. Karst N, Dralle D, Thompson S. 2016 Spiral and rotor patterns produced by fairy ring fungi. *PLoS ONE* **11**, e0149254. (doi:10.1371/journal.pone.0149254)
58. Dahlberg A, Stenlid J. 1995 Spatiotemporal patterns in ectomycorrhizal populations. *Can. J. Bot.* **73**, 1222–1230. (doi:10.1139/b95-382)
59. Pickard BG. 1973 Action potentials in higher plants. *Bot. Rev.* **39**, 172–201. (doi:10.1007/BF02859299)
60. Belousov BP. 1959 A periodic reaction and its mechanism. *Compil. Abstr. Radiat. Med.* **147**, 1.
61. Zhabotinsky AM. 1964 Periodic processes of malonic acid oxidation in a liquid phase. *Biofizika* **9**, 11.
62. Kuhnert L. 1986 A new optical photochemical memory device in a light-sensitive chemical active medium. *Nature* **319**, 393–394. (10.1038/319393a0)
63. Kuhnert L, Agladze KI, Krinsky VI. 1989 Image processing using light-sensitive chemical waves. *Nature* **337**, 244–247.
64. Kaminaga A, Vanag VK, Epstein IR. 2006 A reaction–diffusion memory device. *Angew. Chem. Int. Edn* **45**, 3087–3089. (doi:10.1002/anie.200600400)
65. Steinbock O, Kettunen P, Showalter K. 1996 Chemical wave logic gates. *J. Phys. Chem.* **100**, 18 970–18 975. (doi:10.1021/jp961209v)
66. Sielewiesiuk J, Górecki J. 2001 Logical functions of a cross junction of excitable chemical media. *J. Phys. Chem. A* **105**, 8189–8195. (doi:10.1021/jp011072v)
67. Steinbock O, Tóth Á, Showalter K. 1995 Navigating complex labyrinths: optimal paths from chemical waves. *Science* **267**, 868–871. (doi:10.1126/science.267.5199.868)
68. Rambidi NG, Yakovenchuk D. 2001 Chemical reaction-diffusion implementation of finding the shortest paths in a labyrinth. *Phys. Rev. E* **63**, 026607. (doi:10.1103/PhysRevE.63.026607)
69. Adamatzky A, de Lacy Costello B. 2002 Collision-free path planning in the Belousov-Zhabotinsky medium assisted by a cellular automaton. *Naturwissenschaften* **89**, 474–478. (doi:10.1007/s00114-002-0363-6)
70. Gorecki J, Gorecka JN, Adamatzky A. 2014 Information coding with frequency of oscillations in Belousov-Zhabotinsky encapsulated disks. *Phys. Rev. E* **89**, 042910. (doi:10.1103/PhysRevE.89.042910)
71. Adamatzky A, de Lacy Costello B, Melhuish C, Ratcliffe N. 2004 Experimental implementation of mobile robot taxis with onboard Belousov–Zhabotinsky chemical medium. *Mater. Sci. Eng. C* **24**, 541–548. (doi:10.1016/j.msec.2004.02.002)
72. Yokoi H, Adamatzky A, de Lacy Costello B, Melhuish C. 2004 Excitable chemical medium controller for a robotic hand: closed-loop experiments. *Int. J. Bifurcation Chaos* **14**, 3347–3354. (doi:10.1142/S0218127404011363)
73. Vazquez-Otero A, Faigl J, Duro N, Dormido R. 2014 Reaction-diffusion based computational model for autonomous mobile robot exploration of unknown environments. *IJUC* **10**, 295–316. (doi:10.1017/S1744552314000135)
74. Agladze K, Aliev RR, Yamaguchi T, Yoshikawa K. 1996 Chemical diode. *J. Phys. Chem.* **100**, 13 895–13 897. (doi:10.1021/jp9608990)
75. Igarashi Y, Gorecki J. 2011 Chemical diodes built with controlled excitable media. *IJUC* **7**, 141–158.
76. Gorecki J, Natalia Gorecka J. 2006 Information processing with chemical excitations–from instant machines to an artificial chemical brain. *Int. J. Unconventional Comput.* **2**, 36–48.
77. Stovold J, O'Keefe S. 2012 Simulating neurons in reaction-diffusion chemistry. In *Int. Conf. on Information Processing in Cells and Tissues* (eds MA Lones, SL Smith, S Teichmann, F Naef, A Jonsson, MA Trefzer), pp. 143–149. Berlin, Germany: Springer.
78. Luigi Gentili P, Horvath V, Vanag VK, Epstein IR. 2012 Belousov-Zhabotinsky 'chemical neuron' as a binary and fuzzy logic processor. *IJUC* **8**, 177–192.
79. Takigawa-Imamura H, Motoike IN. 2011 Dendritic gates for signal integration with excitability-dependent responsiveness. *Neural. Netw.* **24**, 1143–1152. (doi:10.1016/j.neunet.2011.05.003)
80. Gruenert G, Gizynski K, Escuela G, Ibrahim B, Gorecki J, Dittrich P. 2015 Understanding networks of computing chemical droplet neurons based on information flow. *Int. J. Neural. Syst.* **25**, 1450032. (doi:10.1142/s0129065714500324)
81. Stovold J, O'Keefe S. 2016 Reaction–diffusion chemistry implementation of associative memory neural network. *Int. J. Parallel Emergent Distrib. Syst.* **32**, 74–94. (doi:10.1080/17445760.2016.1155579)
82. Stovold J, O'Keefe S. 2017 Associative memory in reaction-diffusion chemistry. In *Advances in unconventional computing* (ed. A Adamatzky), pp. 141–166. Berlin, Germany: Springer.
83. Gorecki J, Yoshikawa K, Igarashi Y. 2003 On chemical reactors that can count. *J. Phys. Chem. A* **107**, 1664–1669. (doi:10.1021/jp021041f)

84. Yoshikawa K, Motoike I, Ichino T, Yamaguchi T, Igarashi Y, Gorecki J, Natalia Gorecka J. 2009 Basic information processing operations with pulses of excitation in a reaction-diffusion system. *IJUC* **5**, 3–37.
85. Escuela G, Gruenert G, Dittrich P. 2014 Symbol representations and signal dynamics in evolving droplet computers. *Nat. Comput.* **13**, 247–256. (doi:10.1007/s11047-013-9384-7)
86. Gruenert G, Gizynski K, Escuela G, Ibrahim B, Gorecki J, Dittrich P. 2014 Understanding networks of computing chemical droplet neurons based on information flow. *Int. J. Neural. Syst.* **25**, 1450032. (doi:10.1142/s0129065714500324)
87. Gorecki J, Gizynski K, Guzowski J, Gorecka JN, Garstecki P, Gruenert G, Dittrich P. 2015 Chemical computing with reaction–diffusion processes. *Phil. Trans. R. Soc. A* **373**, 20140219. (doi:10.1098/rsta.2014.0219)
88. Adamatzky A, de Lacy Costello B. 2007 Binary collisions between wave-fragments in a sub-excitable Belousov–Zhabotinsky medium. *Chaos Solitons Fractals* **34**, 307–315. (doi:10.1016/j.chaos.2006.03.095)
89. Toth R, Stone C, de Lacy Costello B, Adamatzky A, Bull L. 2010 Simple collision-based chemical logic gates with adaptive computing. In *Theoretical and technological advancements in nanotechnology and molecular computation: interdisciplinary gains: interdisciplinary gains* (ed. B MacLennan), p. 162. Hershey, PA: IGI Global.
90. Adamatzky A, De Lacy Costello B, Bull L, Holley J. 2011 Towards arithmetic circuits in sub-excitable chemical media. *Isr. J. Chem.* **51**, 56–66. (doi:10.1002/ijch.201000046)
91. de Lacy Costello B, Toth R, Stone C, Adamatzky A, Bull L. 2009 Implementation of glider guns in the light-sensitive Belousov-Zhabotinsky medium. *Phys. Rev. E* **79**, 026114. (doi:10.1103/PhysRevE.79.026114)
92. Toth R, Stone C, Adamatzky A, de Lacy Costello B, Bull L. 2009 Experimental validation of binary collisions between wave fragments in the photosensitive Belousov–Zhabotinsky reaction. *Chaos Solitons Fractals* **41**, 1605–1615. (doi:10.1016/j.chaos.2008.07.001)
93. Adamatzky A. 2010 Slime mould logical gates: exploring ballistic approach. (http://arxiv.org/abs/1005.2301)
94. De Lacy Costello B, Adamatzky A, Jahan I, Zhang L. 2011 Towards constructing one-bit binary adder in excitable chemical medium. *Chem. Phys.* **381**, 88–99. (doi:10.1016/j.chemphys.2011.01.014)
95. Sun M-Z, Zhao X. 2013 Multi-bit binary decoder based on Belousov-Zhabotinsky reaction. *J. Chem. Phys.* **138**, 114106. (doi:10.1063/1.4794995)
96. Zhang G-M, Wong I, Chou M-T, Zhao X. 2012 Towards constructing multi-bit binary adder based on Belousov-Zhabotinsky reaction. *J. Chem. Phys.* **136**, 164108. (doi:10.1063/1.3702846)
97. Sun M-Z, Zhao X. 2015 Crossover structures for logical computations in excitable chemical medium. *Int. J. Unconventional Comput.* **11**, 165–184.
98. Guo S, Sun M-Z, Han X. 2015 Digital comparator in excitable chemical media. *Int. J. Unconventional Comput.* **11**, 131–145.
99. Gorecka J, Gorecki J. 2003 T-shaped coincidence detector as a band filter of chemical signal frequency. *Phys. Rev. E* **67**, 067203. (doi:10.1103/PhysRevE.67.067203)
100. Igarashi Y, Gorecki J, Gorecka JN. 2006 Chemical information processing devices constructed using a nonlinear medium with controlled excitability. In *Unconventional computation* (ed. A Adamatzky), pp. 130–138. Berlin, Germany: Springer.
101. Adamatzky A, de Lacy Costello B, Bull L. 2011 On polymorphic logical gates in subexcitable chemical medium. *Int. J. Bifurcation Chaos* **21**, 1977–1986. (doi:10.1142/S0218127411029574)
102. Stevens WM, Adamatzky A, Jahan I, de Lacy Costello B. 2012 Time-dependent wave selection for information processing in excitable media. *Phys. Rev. E* **85**, 066129. (doi:10.1103/PhysRevE.85.066129)
103. Cole L, Orlovich DA, Ashford AE. 1998 Structure, function, and motility of vacuoles in filamentous fungi. *Fungal Genet. Biol.* **24**, 86–100. (doi:10.1006/fgbi.1998.1051)
104. Goldstein RE, Tuval I, van de Meent J-W. 2008 Microfluidics of cytoplasmic streaming and its implications for intracellular transport. *Proc. Natl Acad. Sci. USA* **105**, 3663–3667. (doi:10.1073/pnas.0707223105)
105. Adamatzky A, Schubert T. 2014 Slime mold microfluidic logical gates. *Mater. Today* **17**, 86–91. (doi:10.1016/j.mattod.2014.01.018)
106. Bahn Y-S, Xue C, Idnurm A, Rutherford JC, Heitman J, Cardenas ME. 2007 Sensing the environment: lessons from fungi. *Nat. Rev. Microbiol.* **5**, 57–69. (doi:10.1038/nrmicro1578)
107. Whiting JGH, Jones J, Bull L, Levin M, Adamatzky A. 2016 Towards a Physarum learning chip. *Sci. Rep.* **6**, 19948. (doi:10.1038/srep19948)
108. Trinci APJ. 1974 A study of the kinetics of hyphal extension and branch initiation of fungal mycelia. *Microbiology* **81**, 225–236. (doi:10.1099/00221287-81-1-225)
109. Fromm J, Lautner S. 2007 Electrical signals and their physiological significance in plants. *Plant Cell Environ.* **30**, 249–257. (doi:10.1111/j.1365-3040.2006.01614.x)
110. Van Aarle IM, Axel Olsson P, Söderström B. 2002 Arbuscular mycorrhizal fungi respond to the substrate ph of their extraradical mycelium by altered growth and root colonization. *New Phytologist* **155**, 173–182. (doi:10.1046/j.1469-8137.2002.00439.x)
111. Kung C. 2005 A possible unifying principle for mechanosensation. *Nature* **436**, 647–654. (doi:10.1038/nature03896)
112. Fomina M, Ritz K, Gadd GM. 2000 Negative fungal chemotropism to toxic metals. *FEMS. Microbiol. Lett.* **193**, 207–211. (doi:10.1111/j.1574-6968.2000.tb09425.x)
113. Bahn Y-S, Mühlschlegel FA. 2006 CO_2 sensing in fungi and beyond. *Curr. Opin. Microbiol.* **9**, 572–578. (doi:10.1016/j.mib.2006.09.003)
114. Oh K-B, Nishiyama T, Sakai E, Matsuoka H, Kurata H. 1997 Flow sensing in mycelial fungi. *J. Biotechnol.* **58**, 197–204. (doi:10.1016/s0168-1656(97)00147-8)
115. Jaffe MJ, Leopold AC, Staples RC. 2002 Thigmo responses in plants and fungi. *Am. J. Bot.* **89**, 375–382. (doi:/10.3732/ajb.89.3.375)
116. Howitz KT, Sinclair DA. 2008 Xenohormesis: sensing the chemical cues of other species. *Cell* **133**, 387–391. (doi:10.1016/j.cell.2008.04.019)
117. Rundel PW, Graham EA, Allen MF, Fisher JC, Harmon TC. 2009 Environmental sensor networks in ecological research. *New Phytologist* **182**, 589–607. (doi:10.1111/j.1469-8137.2009.02811.x)
118. Schloter M, Nannipieri P, Sørensen SJ, Dirk van Elsas J. 2018 Microbial indicators for soil quality. *Biol. Fertil. Soils* **54**, 1–10. (doi:10.1007/s00374-017-1248-3)
119. Vogt KA, Publicover DA, Bloomfield J, Perez JM, Vogt DJ, Silver WL. 1993 Belowground responses as indicators of environmental change. *Environ. Exp. Bot.* **33**, 189–205. (doi:10.1016/0098-8472(93)90065-N)
120. Whiting JGH, de Lacy Costello BPJ, Adamatzky A. 2014 Slime mould logic gates based on frequency changes of electrical potential oscillation. *Biosystems* **124**, 21–25. (doi:10.1016/j.biosystems.2014.08.001)
121. Borresen J, Lynch S. 2012 Oscillatory threshold logic. *PLoS ONE* **7**, e48498. (doi:10.1371/journal.pone.0048498)
122. Toussaint GT. 1980 The relative neighbourhood graph of a finite planar set. *Pattern. Recognit.* **12**, 261–268. (doi:10.1016/0031-3203(80)90066-7)